Available online at www.sciencedirect.com

SCIENCE DIRECT®

Polymer 44 (2003) 3745–3752

polymer

www.elsevier.com/locate/polymer

Free energy and confinement force of macromolecules in a slit at full equilibrium with a bulk solution

Tomáš Bleha*, Peter Cifra

Department of Molecular Thermodynamics, Polymer Institute SAV, Slovak Academy of Sciences, Dubravska cesta 9, 84236 Bratislava, Slovakia

Received 13 March 2003; received in revised form 3 April 2003; accepted 3 April 2003

Abstract

Nondilute athermal and theta solutions of nonadsorbing flexible macromolecules in equilibrium with repulsive slit-like pores were examined by the lattice Monte Carlo simulations. The free energy of confinement $\Delta A/kT$ and the force f/kT exerted by polymers on the slit were computed as a function of the slit width D in a wide range of bulk concentrations ϕ. The free energy and force profiles in nondilute solutions were found to deviate considerably from the ideal chain theory; the perturbation of chains by a presence of the slit walls were substantially reduced in nondilute solutions. The free energy and force functions appropriate for nondilute solutions were derived by fitting the simulation data. Further, the relative pressure p_I/p_E exerted by the nonadsorbing confined molecules on the slit walls was calculated. The depletion effect relevant to colloid stabilization was found in dilute solutions to be slightly weaker for excluded-volume chains than for ideal chains. The relative pressure equation was modified to cover semidilute solutions, by using the mean-field and scaling expressions of the osmotic pressure. Both the relative pressure p_I/p_E and the intra-slit concentration profiles $\phi_I(x)$ in tandem display a suppression of the depletion effect with increasing ϕ in simidilute solutions.

Keywords: Confined excluded-volume chains; Semidilute solutions; Depletion effect

---

1. Introduction

Confinement of polymers by interfaces is of importance in context of colloid stabilization, polymer adhesion and lubrication, polymer intercalation, biopolymers at cell membranes, etc. In theory and simulations the confining boundary is frequently modelled by a slit formed by two infinite parallel planes. For a polymer solution in a slit two thermodynamic conditions should be distinguished as the separation D of slit plates is varied [1]: (a) the number of polymer chains in a solution between plates remains constant during the slit compression or expansion, or (b) the free exchange of polymer molecules between confined and bulk solutions at equilibrium is allowed. These closed and open system situations are referred to as the restricted and full equilibrium cases, respectively [1].

The model of slit-like pore in equilibrium with bulk solution corresponds to many practically important cases when a nonadsorbing polymer solution fills up pores in chromatographic or membrane separation media or contains colloidal particles. Monte Carlo (MC) simulations on a lattice have been used to examine single athermal chains confined in a slit with hard (repulsive) walls. The athermal chain properties investigated include the end-to-end distance and the radius of gyration R_g [2–5], chain elasticity [3] and the free energy of confinement ΔA_0 [5–7]. In open systems the free energy is related to the partition coefficient K_0 at infinite dilution, $\Delta A_0 = -kT \ln K_0$, where $K_0 = \phi_I/\phi_E$ and ϕ_I and ϕ_E are volume fractions of a polymer in a slit and in bulk solution, respectively. In this way the free energy ΔA_0 was also calculated for single theta chains [7]. The dependences of ΔA_0 and K_0 on the molecule-to-slit size ratio $2R_g/D$ obtained from simulations of excluded volume chains were compared with the rigorous analytical relation formulated for ideal (Gaussian) chains [8] and small deviations were noticed [7]. In the narrow slit limit $D \ll R_g$ the scaling theory [9,10] provides a semiquantitative prediction of the free energy ΔA_0 for both athermal and theta chains.

In nondilute polymer solutions, simulations under full equilibrium conditions have shown that an increase in the

---

* Corresponding author. Tel.: +4212-54777414; fax: +4212-54775923.
E-mail address: upoltble@savba.sk (T. Bleha).

0032-3861/03/$ - see front matter © 2003 Elsevier Science Ltd. All rights reserved.
doi:10.1016/S0032-3861(03)00290-8

concentration ϕ of the polymer in the bulk solution augments the partition coefficient K above its value in the dilute limit K_0 [6,7,11–14]. A transition [10] from a weak to a strong penetration of chains into a repulsive slit was observed in simulations in semidilute athermal solutions [6]. The change of solvent quality to the theta state brings about a qualitative change of behaviour: the weak-to-strong penetration transition is delayed to much higher concentrations. In the theta solvent repulsion between chains pushing them into pores becomes effective at higher concentrations than in good solvents [11]. The concentration effects on K were also studied in solutions of polymer mixtures with the aim to develop an effective technique for separation of macromolecules at higher concentrations [12]. The available variations of K with bulk concentration ϕ can be easily recast into dependences of the free energy ΔA on ϕ.

The confinement force, a quantity closely related to ΔA, can be deduced from simulations as well. It is defined as the derivative $f/kT = -\mathrm{d}(\Delta A/kT)/\mathrm{d}D$ and was previously calculated for single athermal chains in a repulsive slit at restricted [15,16] and full [17] equilibrium. One can anticipate that the confinement force should depend on bulk concentration and solvent quality in a way similar to the free energy ΔA.

The confinement force f contributes to the pressure p_I exerted by the confined molecules on the walls inside slit [18,19]. Slit walls also experience a pressure p_E from the surrounding bulk solution. The negative value of the net pressure $\Delta p = p_\mathrm{I} - p_\mathrm{E}$ brings about the so-called depletion effect in colloid solutions. This effective attraction between colloidal particles has significant scientific and technological consequences. Analytical relations for the depletion effect in a slit are available only in the case of isolated ideal chains [20].

In the present report lattice Monte Carlo (MC) simulations were performed for a polymer solution in a repulsive slit in a full equilibrium with a bulk. The free energy of confinement ΔA and the confinement force f were calculated as a function of slit width D in athermal and theta solvents in a wide range of polymer concentrations ϕ. The pressure on the slit walls and the depletion effect were evaluated in dilute and semidilute solutions. It was found that the confinement and depletion phenomena are suppressed by the concentration.

2. Simulation method

The simulation set-up was described previously [6,7,11]. Two boxes connected to each other are assumed in simulations on a cubic lattice: the box E, representing the exterior (bulk) phase and the box I, representing the interior slit pore. The box E has dimensions of $50 \times 30 \times 50$ (in lattice units a) along the x, y and z directions, respectively. In the box I of the dimensions $(D+1) \times 30 \times 50$ there are two solid walls at $x = 1$ and at $x = D + 1$ extending in the y and z directions and forming a slit. The width D is defined as the distance between the two lattice layers occupied by solid walls. The polymer beads are not allowed to occupy the sites on solid walls. Periodic boundary conditions apply to all pairs of opposite walls in the boxes except two solid walls.

Self-avoiding walks consisting of $N = 100$ beads in each chain were generated on the cubic lattice. The athermal model with zero value of the reduced contact energy $\epsilon_\mathrm{S} = e_\mathrm{S}/kT$, where e_S is the segment contact energy and kT the thermal energy, represents the good solvent condition. Theta chains were generated by using $\epsilon_\mathrm{S} = -0.2693$ for both intra- and inter-molecular nonbonded contacts [21].

Chains were equilibrated using the reptation moves and the Metropolis algorithm. The simulations provide the equilibrium concentrations of the chains exchanged between the bulk and the slit without the need to calculate the confinement free energy from the respective chemical potentials. The overall thermodynamic ensemble is canonical and features the aspects known as the Gibbs ensemble, because it is ensured that the chemical potentials of the chains in the slit and in the bulk are equal. The respective final volume fractions in boxes I and E are adjusted after equilibration from the available chains in the system. Their ratio $\phi_\mathrm{I}/\phi_\mathrm{E}$ gives the partition coefficient K and the free energy of confinement $\Delta A = -kT \ln K$. The volume fractions ϕ_E (denoted henceforth also as ϕ where appropriate) up to 0.35 for athermal chains and up to 0.7 for theta chains were used.

The overlap concentration ϕ^*, representing the threshold between dilute and semidilute concentration regimes, was calculated using the relation [11] $\phi^*[2^{1/2}(R_g/a + \alpha)]^3 = N$. Here, the extra constant α accounts for the thickness of a coating needed to translate R_g^3 calculated on the lattice into the volume occupied by the chain in the continuous space. The overlap concentration ϕ^* is 0.120 for athermal chains and 0.207 for theta chains.

The root-mean-square radius of gyration of free unconfined chains of $N = 100$ is $R_g/a = 6.45$ and 5.34 for athermal and theta chains in the dilute solution limit. Simulations were performed for slit widths D/a between 8 and 48. The coil-to-pore size ratio $2R_g/D$ ranged between 0.2 and 1.8 and covered fully the regions of weak ($2R_g/D \ll 1$) and moderate ($2R_g/D \approx 1$) chain confinements.

3. Results and discussion

3.1. Free energy representation

The term ΔA represents the free energy of transfer of a macromolecule from a bulk solution of concentration ϕ to a solution in a slit of concentration ϕ_I. Thus, in repulsive slits the free energy ΔA depends on the plate separation D, concentration ϕ and solvent quality. In theoretical and simulation reports mostly the free energy change of an isolated polymer chain ΔA_0 is considered. For example the analytical theory [8] provides the relations for ΔA_0 in case of freely jointed ideal chains confined in cavities of simple geometries such as slit, cylinder and sphere.

The changes of the free energy ΔA of excluded volume chains with the bulk concentration ϕ were evaluated by simulations of athermal and theta solutions. For a repulsive slit the 3D plot of the free energy $\Delta A/kT$ as a function of the solute-to-pore ratio $2R_g/D$ and concentration ϕ is shown in Fig. 1. It is seen that the free energy penalty $\Delta A/kT$ raises in repulsive slits by increase in confinement $2R_g/D$ mainly due to a loss of conformational entropy of chains in both solvents. However, this confinement penalty diminishes with an increasing concentration ϕ. The concentration dependence of $\Delta A/kT$ in Fig. 1 differs substantially in athermal and theta solvents. This difference can be rationalized in a similar way as the concentration dependence of the partition coefficient K in a repulsive slit [11]. The extent of penetration of coils into a slit is given by a balance of the confinement free energy penalty and the bulk osmotic pressure. At higher ϕ the increasing osmotic pressure (repulsion of coils) effectively pushes the chains into a slit. In good solvents the second osmotic virial coefficient A_2 is large and thus the penalty $\Delta A/kT$ rapidly decreases with ϕ. In contrast, $A_2 = 0$ in a theta solvent and the chains are forced to enter the slit at higher concentrations by a positive third virial coefficient of the bulk solution.

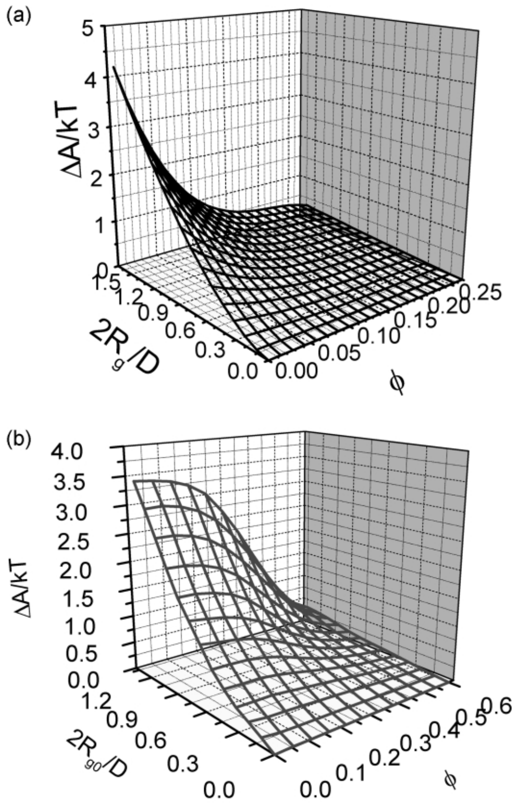

Fig. 1. Free energy of confinement as a function of confinement ratio $2R_g/D$ and bulk concentration ϕ for athermal chains (a) and theta chains (b).

The variation of the confinement free energy $\Delta A/kT$ with the chain-to-pore size ratio $2R_g/D$ in athermal solution is detailed in Fig. 2 for the selected relative concentration $\phi_{\mathrm{rel}} = \phi/\phi^*$. For a given slit width the penalty $\Delta A/kT$ is reduced (the penetration of macromolecules into slit is enhanced) by increasing ϕ. The free energy function for ideal freely jointed chains confined in a slit [8] is also included in Fig. 2. The ideal chain theory [8] predicts the proportionalities $\Delta A_0 \sim D^{-1}$ in wide slits and $\Delta A_0 \sim D^{-2}$ in narrow slits. The scaling theory, applicable only under limiting conditions of narrow pores, suggests the relations $\Delta A_0 \sim D^{-2}$ for theta chains and $\Delta A_0 \sim D^{-5/3}$ for athermal chains [9,10].

Pursuing an analogy with the above theoretical relations we have fitted the simulation data in Fig. 2 by a power function

$$\Delta A/kT = p(2R_g/D)^q \tag{1}$$

where the parameters p and q depend on the concentration ϕ. Using the logarithmic form of the above function the linear fit of the simulation data yields the parameters p and q listed in Tables 1 and 2 for athermal and theta chains, respectively. It should be emphasized that the variables p and q are merely the effective fitting parameters of the free energy function in the range of the confinement ratio $2R_g/D$ considered in the simulations. Thus, the effective exponents q from Tables 1 and 2 pertain to nondilute solutions under weak and moderate chain confinements encountered in numerous scientific and technological applications. In contrast, the exponent q employed by the scaling theory is relevant to the situations of strong chain confinements $2R_g/D \gg 1$. The partitioning of polymers in strongly confined semidilute solutions is controlled by the ratio of the correlation length of monomer density fluctuations ξ to the slit width D and the scaling exponent q in the relation $\Delta A \approx (\xi/D)^q$ is independent of the concentration ϕ [6,11].

The data in Tables 1 and 2 show that the prefactor p and

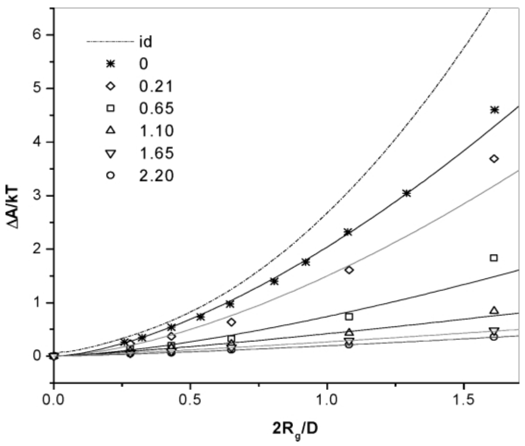

Fig. 2. Free energy of confinement in good solvents as a function of the coil-to-slit size ratio $2R_g/D$ at various reduced bulk concentrations ϕ/ϕ^*.

Table 1
The concentration dependence of the fitting parameters in Eq. (1) for athermal solutions

ϕ	ϕ/ϕ^*	p	q
0	0	2.04	1.57
0.025	0.21	1.50	1.58
0.078	0.65	0.74	1.46
0.132	1.10	0.42	1.23
0.198	1.65	0.27	1.18
0.264	2.20	0.20	1.20

the exponent q are reduced in both solvents by an increase in concentration ϕ. At high concentrations the prefactor p seems to converge to values around 0.2 and the exponent q to values slightly above 1. The concentration dependence of the exponent q is consistent with the simulations of the confined polymer melt where the proportionality $\Delta A \sim D^{-1}$ was inferred for a narrow slit [22]. Clearly, perturbation of chains by a presence of the slit walls is substantially reduced in nondilute solutions relative to the isolated ideal or excluded-volume chains and ultimately in the melt all correlations are quickly shielded.

The confinement penalty $\Delta A/kT$ of the excluded volume chains at various concentrations ϕ is contrasted in Fig. 2 with the corresponding function for an isolated ideal chain. Evidently, the Casassa ideal chain relation is roughly appropriate for excluded volume chains in a very dilute solution only. However, the concentration-independent ideal chain relations for various confining geometries [8] are widely used to estimate the confinement free energy of molecules bounded by the various solid-state structural features such as the layered structures in block copolymers, polymer blends and intercalates, thin films, etc. [23–25]. Clearly, such a practice results in a considerable overestimation of the confinement penalty $\Delta A/kT$, particularly when the size of a molecule and a slit becomes comparable [26]. As a substitute, the fit of simulation data by Eq. (1), with parameters summarized in Tables 1 and 2, can be utilized for this purpose. For example, these results can be used in the mean-field model of thermodynamics of intercalation into organically modified layered silicates [25], instead of the approximate random-flight-chain relation originally employed.

Table 2
The concentration dependence of the fitting parameters in Eq. (1) for theta solutions

ϕ	ϕ/ϕ^*	p	q
0	0	2.22	1.65
0.1	0.48	2.17	1.59
0.2	0.97	1.99	1.71
0.3	1.45	1.45	1.70
0.4	1.93	0.89	1.59
0.5	2.42	0.47	1.30
0.6	2.90	0.27	1.16

An approximate treatment of the chemical potential μ_{I} of a polymer solution in a repulsive slit is also based on the concentration-independent free energy of confinement ΔA_0. In general, the intra-pore chemical potential $\mu_{\mathrm{I}}(\phi_{\mathrm{I}}, D)$ is a function of concentration ϕ_{I} and pore width D. It can be approximately resolved into two terms, each depending on a single variable only [6,14,17]

$$\mu_{\mathrm{I}}(\phi_{\mathrm{I}}, D) = \mu_{\mathrm{I}}(\phi_{\mathrm{I}}, \infty) + \mu_{\mathrm{I}}(0, D) \tag{2}$$

where the first term on the right-hand side accounts for the concentration dependence of unconfined solution and the second term is identical to the free energy of confinement of an isolated chain ΔA_0.

3.2. Confinement force

By the differentiation of the free energy data according to D, a closely associated function, variation of the confinement force f/kT (in units a^{-1}) with the plate separation D was evaluated. This dependence is plotted in Figs. 3 and 4 for several concentrations ϕ in athermal and theta solvents, respectively. It is seen that in both solvents the confinement force decreases monotonically with increasing separation D (normalized by the coil diameter $2R_g$). However, the repulsive nature of the steric force markedly diminishes in semidilute solutions. The confinement force obtained by simulation under restricted equilibrium conditions using the isolated bead-spring chains [15] is also included in Fig. 3. The data shown correspond to the chain lengths $N = 128$ and 256 and to slit widths between 8 and 32. No essential differences are noticeable in Fig. 3 among confinement force f/kT determined in the dilute solution limit under restricted and full equilibrium conditions.

Considerable differences are observed between two solvents as regards to the influence of concentration ϕ on the plots f/kT versus $D/2R_g$: in the athermal solvent a strong reduction in force occurs at ϕ below the overlap

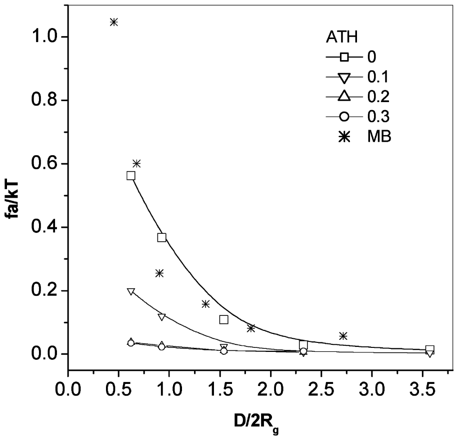

Fig. 3. Plot of the reduced confinement force f/kT (in lattice modulus units) of athermal chains as a function of the normalized separation of repulsive walls $D/2R_g$ at indicated bulk volume fractions ϕ. Star symbols represent the data from simulations under restricted equilibrium conditions [15].

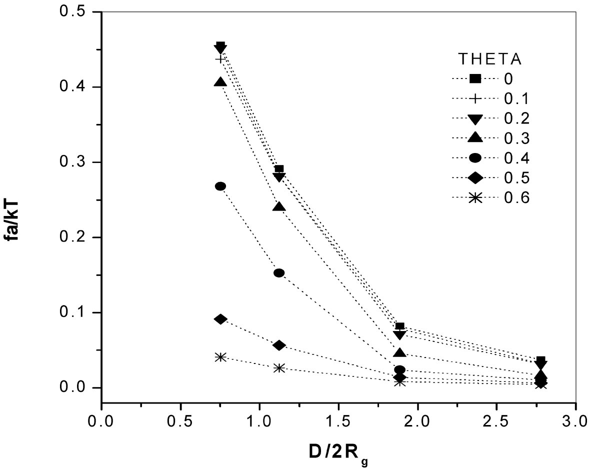

Fig. 4. Plot of the reduced force f/kT (in lattice modulus units) as a function of the slit width $D/2R_g$ at bulk volume fractions ϕ of the theta solutions indicated in the legend.

concentration $\phi^* = 0.12$; the confinement force almost vanishes for $\phi > 0.2$. In the theta solvent, only minor changes in the f/kT values are seen in the dilute solution range by an increase in the concentration to about $\phi = 0.3$; subsequently, f/kT is substantially reduced.

The differentiation of the Eq. (1) according to D yields the following power-law function for the confinement force $f(D, \phi)$

$$f/kT = pq(2R_g)^q D^{-q-1} \tag{3}$$

The parameters p and q from Tables 1 and 2 can be employed to represent the concentration-dependent confinement force in the range of confinement investigated. The effective exponent $r = -q - 1$ of the relationship $f/kT \sim D^r$ attains the values between -2.57 and -2.18 for athermal chains and between -2.65 and -2.16 for theta chains within the concentration ranges used. For ideal chains the relations $f \sim D^{-2}$ in the wide slits and $f \sim D^{-3}$ in the narrow slits follow from theory [8]. Again, these data reveal that the confinement force, one of the manifestations of the confined chain behaviour, is suppressed by increasing concentration of a polymer in a solution, by a mechanism resembling the screening of the excluded volume in the unconfined concentrated solutions.

In the strong confinement region ($2R_g/D \gg 1$), not covered by our simulations, the scaling theory [9] provides the scaling relations for confinement force. These relations were tested in previous simulations of athermal chains trapped in a slit [15–17]. Although overall agreement was found, the difference close to 10% between simulations and theoretical prediction was noted. For example the exponent r, instead of $r = -2.68$, appeared to reach -2.41 at large chain lengths [16]. Moreover, it should be pointed out that the correction for the penetration length γ should be allowed for in expressing the distance of monomers to the wall [28] when lattice simulations are linked with the scaling theory developed for a continuous medium.

The scaling theory arguments [10,27] can be exploited to deduce the scaling relations for the confinement force in a semidilute solution in narrow repulsive slits. In athermal solution the correlation length ξ is given as $\xi = R_g(\phi/\phi^*)^{-3/4}$ and the free energy scales as $\Delta A \cong (\xi/D)^{5/3} = \phi^{-5/4}D^{-5/3}$. The relation $f \cong \phi^{-5/4}D^{-8/3}$ follows by differentiation according to D. Similarly, in theta solutions $\xi \cong a\phi^{-1}$ [11] and $\Delta A \cong (\xi/D)^2 = (\phi D)^{-2}$. Then the force is given as $f \cong \phi^{-2}D^{-3}$. Hence, above scaling relations confirm that the confinement force diminishes by increasing concentration and this reduction is controlled in athermal and theta solutions by different functions of ϕ.

3.3. Pressure on the wall

The confinement force f contributes to the pressure $p_I = -(dA/dV)_T$ exerted by the confined molecules on the walls inside a slit. The slit walls also experience a pressure p_E from the surrounding bulk solution. Information from simulations on the pressure p_I and p_E is relevant to the problem of stability of colloidal dispersions. Addition of nonadsorbing polymers to a stable solution of colloid particles results in polymer-mediated 'depletion' interaction arising from unbalanced pressures inside the slit and in the bulk [1,18,19]. At full equilibrium conditions polymer molecules move out of the gap between the colloid particle surfaces, into bulk solution. The negative value of the net pressure $\Delta p = p_I - p_E$ brings about the depletion effect i.e. effective attraction between colloidal particles.

The pressure p_I in dilute polymer solutions where the interchain interactions are negligible is related to the confinement force as [18,19]

$$p_I = (kTn_I/V_I)(1 + Df/kT) = \pi_I^{id}(1 + Df/kT) \tag{4}$$

where n_I/V_I is the molecular concentration (number density) of a polymer within a slit and π^{id} is the osmotic pressure of ideal solution. In narrow slits $Df/kT \gg 1$ in dilute solutions (Figs. 3 and 4) and the confinement force term is the leading term in Eq. (4). The term Df/kT can formally be regarded as an increase in the effective number of molecules in the slit that produce the pressure p_I. In contrast, in wide slits and nondilute solutions the contribution of the term Df/kT to the pressure p_I may be small.

The external pressure p_E on slit walls in dilute solution is determined by the osmotic pressure term π_E^{id}. In the lattice mean-field theory of polymer solution the ideal osmotic pressure is specified by the relation [27]

$$\pi^{id} = (n_{site}\phi/NV)kT \tag{5}$$

where n_{site} is the number of lattice sites, N is the number of polymer beads and V volume of solution.

From the above relations the ratio of intra-pore and bulk pressure in dilute solutions can be expressed

$$p_I/p_E = (\pi_I^{id}/\pi_E^{id})[1 + Df/kT] = K[1 + Df/kT]$$
$$= K + D(dK/dD) \qquad (6)$$

Analytical results on the variation of the ratio p_I/p_E with the slit plate separation D under full equilibrium conditions were reported for a solution of ideal polymers [20]. The corresponding data on the relative pressure p_I/p_E of excluded-volume chains from simulation of dilute athermal and theta solutions are shown in Fig. 5. It is seen that due to expulsion of molecules from the slit the intra-slit pressure drops significantly below the bulk pressure at the wall separations less than about $3R_g$. The depletion effect becomes weaker in the excluded-volume chains relative to ideal chains but no difference in this respect is observed between athermal and theta chains in this reduced plot. An increase in concentration of theta chains to $\phi = 0.2$, still in the dilute solution regime, reduces the depletion effect. The depletion attraction in systems of nonadsorbing polymers is very small compared to adsorbing polymers and notoriously difficult to measure. However, depletion attraction of the type shown in Fig. 5 was observed in recent experiments by the surface force apparatus [29] and AFM technique [30].

To calculate the relative pressure p_I/p_E in nondilute solutions from the simulation data we attempted a simple semiempirical modification of Eq. (6) by dropping the condition of ideality in the ratio of osmotic pressures. The nonideal solution ratio π_I/π_E can be determined by means of mean-field or scaling theories. The mean-field expression reads [27]

$$\frac{\pi V}{n_{site}kT} = \frac{\phi}{N} - \ln(1-\phi) - \phi - \chi\phi^2 \qquad (7)$$

where the Flory–Huggins interaction parameter $\chi = 0$ and 0.5 in athermal and theta solutions, respectively.

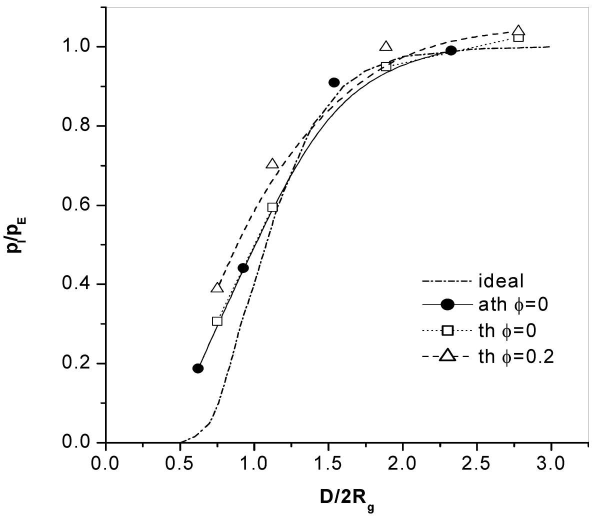

Fig. 5. The dependence of the relative pressure p_I/p_E of macromolecules on the normalized slit width for ideal chains, athermal and theta chains at the dilute solution limit and for theta chains at concentration $\phi = 0.2$.

The ratio of osmotic pressures π_I/π_E calculated by Eq. (7) as a function of concentration ϕ for the slit width $D = 12$ in athermal and theta solutions is shown in Fig. 6. The osmotic pressure in nondilute solutions is higher than in the ideal solution due to additional terms on the right hand-side of the Eq. (7). In athermal solutions the nonideality enhancement of osmotic pressure is more intense for the bulk term than for the intra-pore term. Therefore, the ratio π_I/π_E for athermal solutions calculated by Eq. (7) shows a less steep rise with concentration in Fig. 6 than the ratio $\pi_I^{id}/\pi_E^{id} = K$ in the ideal solution. In theta solvents the nonideality contributions again reduce the term π_I/π_E relative to the ideal value. In this case the plot of π_I/π_E even shows a minimum, the behaviour apparently connected to the vanishing virial coefficient A_2.

An alternative expression of the osmotic pressure of semidilute solutions based on the blob concept is provided by the scaling theory [10,27]

$$\pi \cong \pi^{id}(\phi/\phi^*)^{5/4} \qquad (8)$$

Again, the osmotic pressure predicted by Eq. (8) in semidilute solutions is much larger than one would find for the ideal solution at the same concentration. Using Eq. (8) the ratio π_I/π_E can be conveniently expressed as

$$\pi_I/\pi_E \cong K^{9/4} \qquad (9)$$

The variation of π_I/π_E with concentration ϕ calculated by Eq. (9) for the slit width $D = 12$ in athermal and theta solutions is also shown in Fig. 6. It is seen that in athermal solutions both scaling and mean-field theories provide very similar dependences of π_I/π_E versus ϕ that converge at higher concentrations. On the contrary, the scaling and mean-field functions in theta solutions differ in the whole concentration range.

The scaling relation (9) was used to modify Eq. (6) to be

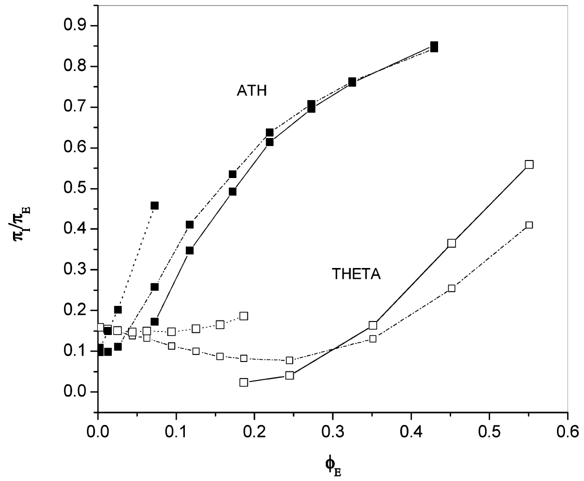

Fig. 6. Plot of the ratio of osmotic pressure π_I/π_E inside and outside the slit as a function of bulk concentration ϕ in athermal (full symbols) and theta solutions (open symbols). Computations for ideal dilute solutions (dotted lines), by the mean-field relation Eq. (7) (dashdot lines) and by the scaling relation Eq. (9) for the semidilute region (full lines).

applicable to semidilute solutions

$$p_I/p_E = K^{9/4}[1 + Df/kT] \tag{10}$$

The relative net pressure $\Delta p_I/p_E$ was calculated by Eq. (10) using the concentration-dependent values of the partition coefficient K and the confinement force f from simulations. The results for athermal and theta solutions in the concentration ranges of strong intra-slit penetration are shown in Fig. 7. The depletion effect $\Delta p < 0$, i.e. effective attraction of slit walls, is predicted for all curves in Fig. 7. The shift of the depletion region to the smaller separations with increasing ϕ is visible in Fig. 7 in the region of about $D/2R_g < 1.25$. Evidently, the depletion effect diminishes by an increase in concentration and may even disappear when the concentration of athermal solution further increases in Fig. 7. On the other hand, the relative net pressure of theta solutions shows the values below that for ideal chains in Fig. 7 at higher separations. It may indicate either the failure of relation (10) in case of theta chains or a possible inaccuracy of the numerical derivation by which the force data were determined. It should also be mentioned that the above mean-field and scaling calculations of the net pressure neglect an inhomogeneity in the segment distribution in the slit (manifested in the shape of the concentration profile, vide infra).

On the whole, the ratio of osmotic pressure π_I/π_E invariably increases with ϕ (Fig. 6) and should converge to unity as ϕ_I moves toward ϕ. Since relative pressure p_I/p_E also approaches unity on increase in ϕ, the term Df/kT in Eq. (6) or (10) must diminish and finally vanish on increase in ϕ. That is exactly the behaviour of the repulsive confinement force observed in Figs. 3 and 4.

In addition to the confinement force and net pressure, the concentration profiles $\phi_I(x)$ across the slit provide the readily discernible demonstration of the depletion effect. The concentration profiles normalized by the bulk concentration $\phi_I(x)/\phi$ from simulations of athermal solutions in the slit of width $D = 12$ are plotted in Fig. 8. The depletion layer thickness is gradually reduced on increasing ϕ, in a complete correspondence to the reduction of the depletion effect in plots of $\Delta p/p_E$ in Fig. 7 and the reduction of confinement force by ϕ in Figs. 3 and 4.

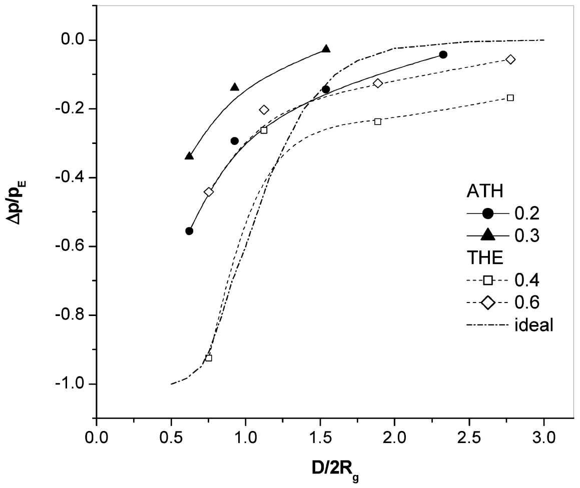

Fig. 7. Plot of the relative pressure $(p_I - p_E)/p_E$ versus the normalized slit width calculated by Eq. (10) for semidilute solutions of athermal chains (full lines) and theta chains (dashed lines) at concentrations indicated. The dashdot line represents the ideal chain behaviour.

The simulations of short oligomers at constant chemical potential [31] and of bead-spring model chains of lengths $N = 64$ [32] also found a decrease of the depletion effect with an increase in the density of monomers in the system. In these papers [31,32] even the existence of the region of $\Delta p/p_E > 0$ i.e. of weak depletion repulsion at short distances and high densities was conjectured.

Equilibrium distribution of macromolecules between bulk solution and a repulsive slit pore can alternatively be treated as a confined (negative) adsorption. The partition coefficient K can be related to the excess adsorbed amount Γ^{ex} of polymer (relative to bulk) in adsorption or depletion lattice layers near the slit walls [14]

$$\Gamma^{ex} = \phi(K - 1)(D - 1)/2 \tag{11}$$

Consequently, in this option, the relative pressure in Eqs. (6) and (10) can be expressed by means of excess adsorption Γ^{ex} instead of the coefficient K. The adsorbed amount Γ^{ex} can be computed from the respective concentration profile $\phi_I(x)$ and bulk concentration ϕ_E. Closely related approaches, based on excess negative adsorption, were previously used to calculate the depletion interaction potential (an integral of the net pressure) due to theta [1] and ideal [33] nonadsorbing polymers between repulsive plates.

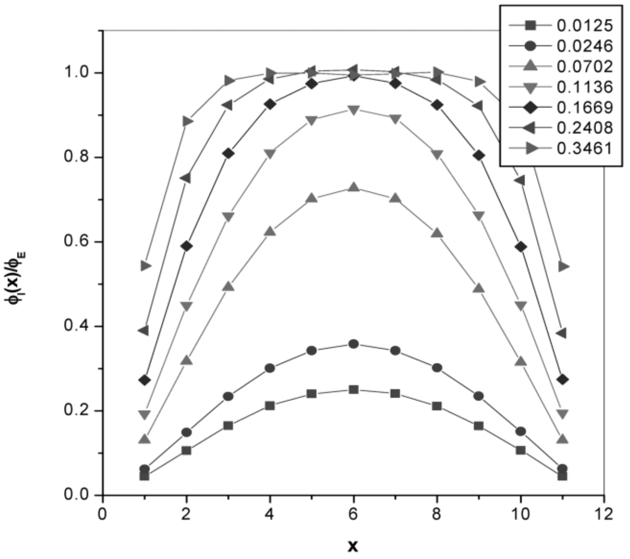

Fig. 8. Normalized concentration profiles $\phi_I(x)/\phi_E$ of athermal chains in the repulsive slit of the width $D = 12$ in equilibrium with the bulk solution of the indicated concentration.

4. Concluding remarks

The influence of polymer concentration on the thermodynamics of polymers confined by repulsive parallel plates was examined by simulations in an open system in good and theta solvents. It was found that the dependences of the confinement free energy $\Delta A/kT$ and the confinement force f/kT on the molecule-to-slit size ratio $2R_g/D$ in nondilute solutions considerably deviate from the theoretical relations for ideal chains. Appropriate functions for nondilute solutions were derived by fitting the simulation data. Repulsive confinement force f/kT was found to decrease with an increasing bulk concentration ϕ. The concentration dependence of the force differs significantly among athermal and theta solutions.

The relative pressure p_I/p_E exerted by the confined molecules on the walls, of vital interest in colloid stabilization, was calculated in dilute solutions. The excluded-volume chains show in dilute solutions a weaker depletion effect than ideal chains. The relationship for the relative pressure p_I/p_E was tentatively extended to semidilute solutions by employing the nonideal osmotic pressures π_I/π_E inside and outside the slit computed by the mean-field and scaling theories. The relative pressure p_I/p_E in semidilute solutions shows the strong decline of the depletion effect with increasing ϕ, with some irregularities in the theta solutions. The intra-slit concentration profiles $\phi_I(x)$ from simulations are consistent with a general trend of suppression of confinement phenomena by increasing the polymer concentration, by a manner comparable to the screening of the chain excluded volume in unconfined concentrated solutions.

Acknowledgements

The research was supported in part by the Grant Agency for Science (VEGA) grants 2/3012/23 and 2/3013/23.

References

[1] Fleer GJ, Cohen Stuart MA, Scheutjens JMHM, Cosgrove T, Vincent B. Polymers at interfaces. London: Chapman & Hall; 1993.

[2] van Vliet JH, Luyten MC, ten Brinke G. Macromolecules 1992;25:3802.

[3] Cifra P, Bleha T. Macromol Theory Simul 1999;8:603.

[4] Wang Y, Teraoka I. Macromolecules 2000;33:3478.

[5] van Giessen AE, Szleifer I. J Chem Phys 1995;102:9069.

[6] Wang Y, Teraoka I. Macromolecules 1997;30:8473.

[7] Cifra P, Bleha T. Macromolecules 2001;34:605.

[8] Casassa EF. J Polym Sci Polym Lett Ed 1967;5:773.

[9] Daoud M, de Gennes PG. J Phys (Paris) 1977;38:85.

[10] de Gennes PG. Scaling concepts in polymer physics. Ithaca, NY: Cornell University Press; 1979.

[11] Cifra P, Bleha T, Wang Y, Teraoka I. J Chem Phys 2000;113:8313.

[12] Wang Y, Teraoka I, Cifra P. Macromolecules 2001;34:127.

[13] Teraoka I, Cifra P. J Chem Phys 2001;115:11362.

[14] Škrinárová Z, Bleha T, Cifra P. Macromolecules 2002;35:8896.

[15] Milchev A, Binder K. Eur Phys J B 2000;13:607.

[16] De Joannis J, Jimenez J, Rajagopalan R, Bitsanis I. Europhys Lett 2000;51:41.

[17] Chen Z, Escobedo FA. Macromolecules 2001;34:8802.

[18] Vrij A. Pure Appl Chem 1976;48:471.

[19] Clark AT, Lal M. J Chem Soc Faraday Trans 2 1981;77:981.

[20] Ennis J, Jönsson B. J Phys Chem B 1999;103:2248.

[21] Panagiotopoulos AZ, Wong V, Floriano MA. Macromolecules 1998;31:912.

[22] Kumar SK, Ausserre D, Vacatello M, Yoon DY. ACS Polym Preprints 1989;30:360.

[23] Tucker PS, Paul DR. Macromolecules 1988;21:2801.

[24] Watanabe H, Matsuyama S, Mizutani Y, Kotaka T. Macromolecules 1995;28:6454.

[25] Vaia RA, Giannelis EP. Macromolecules 1997;30:7990.

[26] Cifra P, Bleha T, Škrinárová Z. Macromol Symp 2003; in press.

[27] Teraoka I. Polymer solutions: an introduction to physical properties. New York: Wiley; 2002.

[28] Teraoka I, Cifra P, Wang Y. Macromolecules 2001;34:7121.

[29] Ruths M, Yoshizawa H, Fetters LJ, Israelichvili JN. Macromolecules 1996;29:7193.

[30] Piech M, Walz JY. J Colloid Interf Sci 2002;253:117.

[31] Broukhno A, Jonsson B, Akesson T. J Chem Phys 2000;113:5493.

[32] Milchev A. Eur Phys J E 2002;8:531.

[33] Tuinier R, Vliegenthart GA, Lekkerkerker HNW. J Chem Phys 2000;113:10786.